STATIC QUARK OPERATORS BASED ON LAPLACIAN EIGENMODES*

Roman Höllwieser

Department of Physics, University of Wuppertal
Gaußstrasse 20, 42119 Wuppertal, Germany

Received 25 January 2023, accepted 1 May 2023, published online 27 October 2023

We investigate a representation of static quark operators based on trial states formed by eigenvector components of the covariant lattice Laplace operator. We present an improved method for computing the static quark–anti-quark potential, we visualize optimal quark–anti-quark creation operators, and show first results of the method applied to hybrid mesons as well as static-light systems.

DOI:10.5506/APhysPolBSupp.16.8-A23

1. The static quark–anti-quark potential

The potential of a static quark–anti-quark pair $V_0(r)$ has always played an important role in Quantum Chromodynamics (QCD). It can be computed via Wilson loops [1] and established an understanding of confinement and its interplay with asymptotic freedom, a central problem of particle physics [2]. Let $\bar{Q}^a(\vec{x}\,)$ denote a static color source with $a = 1, 2, 3$ at spatial position $\vec{x}$. Wilson loops arise from correlations in time of trial states $\bar{Q}(\vec{x}\,)U_s(\vec{x},\vec{y}\,)Q(\vec{y}\,)$ for a static color–anti-color source pair located at spatial positions $\vec{x}$ and $\vec{y}$ respectively. The spatial Wilson line $U_s(\vec{x},\vec{y}\,) = \exp(i\int_{\vec{x}}^{\vec{y}} A_\mu \mathrm{d}x^\mu) = \prod U_\mu$ is a path-ordered product of link variables from $\vec{x}$ to $\vec{y}$. We replace the spatial part of trial states in each time-slice with an alternative operator constructed from eigenmodes $v_i(\vec{x}\,)$ of the three-dimensional gauge-covariant lattice Laplace operator Δ

$$\Phi(\vec{x},\vec{y}\,) \;=\; \bar{Q}(\vec{x}\,)\sum_{i=1}^{N_v}\rho_i^2 v_i(\vec{x}\,)v_i^\dagger(\vec{y}\,)Q(\vec{y}\,)\,, \tag{1}$$

which respects the gauge transformation behavior of the spatial Wilson line and ensures gauge invariance of the trial state. We denote Eq. (1) as a

* Presented at *Excited QCD 2022*, Sicily, Italy, 23–29 October, 2022.

Laplace trial state, where we include a quark profile ρ_i, which modulates the contribution from different eigenmodes. In [3, 4], we reformulated the usual Wilson loops in terms of (temporal) *Laplace trial state correlators*, see figure 1, which can also be interpreted as the spatial correlation of static perambulators

$$\tau_{ij}(\vec{y}, t_0, t_1) = v_i^\dagger(\vec{y}, t_0) U_t(\vec{y}, t_0, t_1) v_j(\vec{y}, t_1)\,, \tag{2}$$

and $\bar{\tau}_{ij}(\vec{x}, t_0, t_1)$. These static quark line operators also manifest the computational advantage of the new method compared to standard Wilson loops, since no stair-like Wilson lines need to be constructed for off-axis spatial correlations.

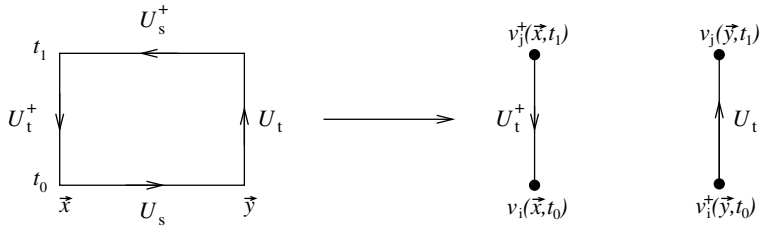

Fig. 1. The spatial Wilson lines $U_s(\vec{x}, \vec{y}, t)$ of the classical Wilson loop $W(R, T)$ of size $(R = |\vec{y} - \vec{x}|) \times (T = |t_1 - t_0|)$ (left) can be replaced by Laplacian eigenvector pairs $v_i(\vec{x}, t) v_i^\dagger(\vec{y}, t)$ (right), to form Laplace trial state correlators via the two static perambulators $\bar{\tau}_{ij}(\vec{x}, t_0, t_1)$ and $\tau_{ij}(\vec{y}, t_0, t_1)$.

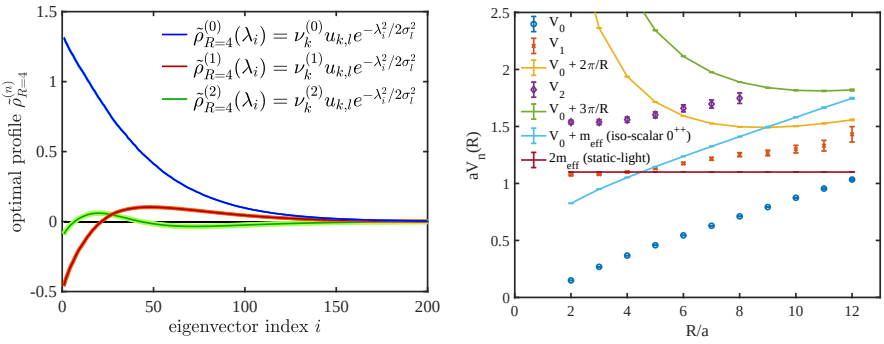

Fig. 2. (Color online) Optimal trial state profiles $\tilde{\rho}^{(n)}_R(\lambda_i)$ (left) and static potentials V_n (right) for ground ($n = 0$, blue) and excited ($n = 1, 2$, red, green/purple) states. u_k and $\nu^{(n)}_k$ are the singular and generalized (eigen-)vectors from a singular value decomposition (SVD) used to prune the original correlation matrix and stabilize the GEVP. We compare with radially excited string states $V_0 + (n+1)\pi/R$, the lowest 0^{++} iso-scalar meson (possible glueball) state $V_0 + m_{\text{eff}}$(iso-scalar 0^{++}) from [5], and two times the static-charm quark mass presented in Section 4.

We improve the operator by introducing a set of Gaussian profile functions into the correlators and solving a generalized eigenvalue problem (GEVP) for the *Laplace trial state correlation matrix* to extract optimal trial state profiles $\tilde{\rho}_i^{(n)}$ for ground and excited states of the static potential $V_n(R)$, $(n = 0, 1, 2)$, see figure 2.

2. Spatial distribution of optimal Laplace trial states

We can visualize the optimal quark–anti-quark creation operators by placing an eigenvector pair $v^\dagger(\vec{z})v(\vec{z})$ which acts as a 'test-charge' in the Laplace trial state

$$\psi^{(n)}(\vec{z}, R) = \left\langle \Big|\Big| \sum_{ij}^{N_v} \tilde{\rho}_R^{(n)}(\lambda_i, \lambda_j) v_i(\vec{x}) v_i^\dagger(\vec{z}) v_j(\vec{z}) v_j^\dagger(\vec{x} + R) \Big|\Big|_2 \right\rangle , \qquad (3)$$

which allows the scanning of individual contributions of the quark–anti-quark operator in a 3D time-slice via the free coordinate $\vec{z}$. We average over the whole lattice $(\vec{x}, t)$, which already gives a very smooth signal on a single configuration. Note that we include the optimal trial state profiles

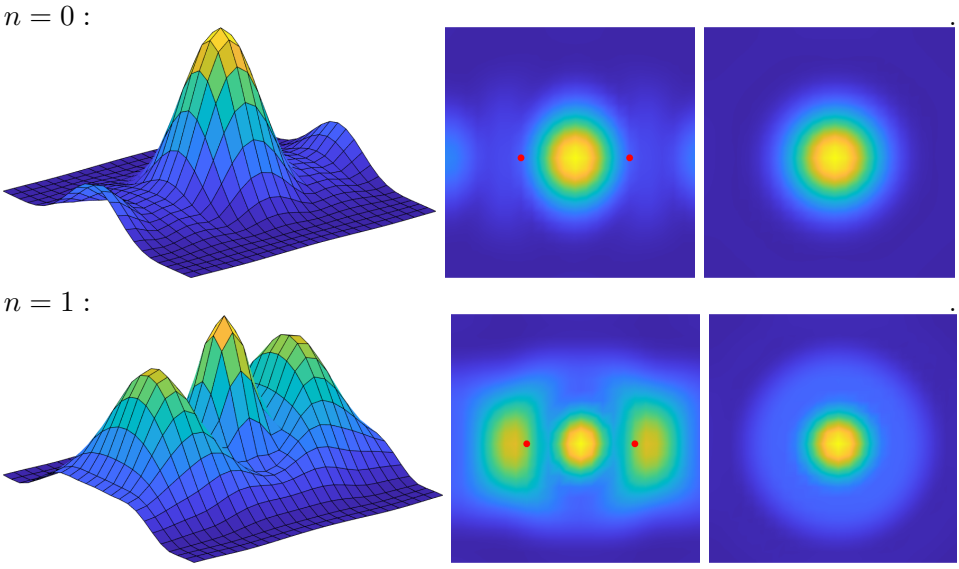

Fig. 3. (Color online) Spatial distribution Eq. (3) along (left, center) and perpendicular to (right) the quark separation ($R = 10a$) axis of the optimal Laplace trial state to measure the ground ($n = 0$, top) and first excited ($n = 1$, bottom) state potential of a static quark–anti-quark pair; the quark locations are indicated by red dots.

$$\tilde{\rho}_R^{(n)}(\lambda_i,\lambda_j) = \sum_{k,l} \nu_k^{(n)} u_{k,l}\, \mathrm{e}^{-\lambda_i^2/4\sigma_l^2}\, \mathrm{e}^{-\lambda_j^2/4\sigma_l^2}\,, \tag{4}$$

which depend on the two eigenvalues λ_i and λ_j. The singular vectors u_k and generalized eigenvectors $\nu^{(n)}$ come from the SVD and GEVP in the static potential calculations for specific quark separation distances R and allow us to look at the flux tube profiles for various energy states of $V_n(R)$, see figure 3.

3. The hybrid static potential of Π_u

Hybrid static potentials can be obtained from correlation functions constructed with Laplace trial states, where the gluonic excitations are realized via covariant derivatives of Laplacian eigenvectors, *e.g.*, for Π_u we could use the operator

$$\begin{aligned}\Pi_u^{mn}(R=|\vec{y}-\vec{x}\,|, T=|t_1-t_0|) = \sum_{i,j,\vec{k}\perp\vec{y}-\vec{x}} \mathrm{e}^{-\lambda_i^2/2\sigma_m^2}\, \mathrm{e}^{-\lambda_j^2/2\sigma_n^2} \\ \left\langle \mathrm{Tr}\Big[U_\mathrm{t}(\vec{x};t_0,t_1) \left\{ \nabla_{\vec{k}} v_j(\vec{x},t_1) v_j^\dagger(\vec{y},t_1) + v_j(\vec{x},t_1) \left[\nabla_{\vec{k}} v_j\right]^\dagger (\vec{y},t_1) \right\} \right. \\ \left. U_\mathrm{t}^\dagger(\vec{y};t_0,t_1) \left\{ \nabla_{\vec{k}} v_i(\vec{y},t_0) v_i^\dagger(\vec{x},t_0) + v_i(\vec{y},t_0) \left[\nabla_{\vec{k}} v_i\right]^\dagger (\vec{x},t_0) \right\} \Big] \right\rangle,\end{aligned} \tag{5}$$

with $\nabla_{\vec{k}} v(\vec{x}) = \frac{1}{2}[U_k(\vec{x}) v(\vec{x}+\hat{k}) - U_k^\dagger(\vec{x}-\hat{k}) v(\vec{x}-\hat{k})]$. One can easily check that this operator is $\mathcal{P}\cdot\mathcal{C}$ negative/odd. Preliminary results of the hybrid static potential for Π_u on a quenched ensemble are presented in the left plot of figure 4, where we use $N_v = 100$ eigenmodes and again solve a GEVP for the correlation matrix of different Gaussian profiles with widths σ_m and σ_n to get optimal profiles $\tilde{\rho}_{\Pi,R}^{(n)}$.

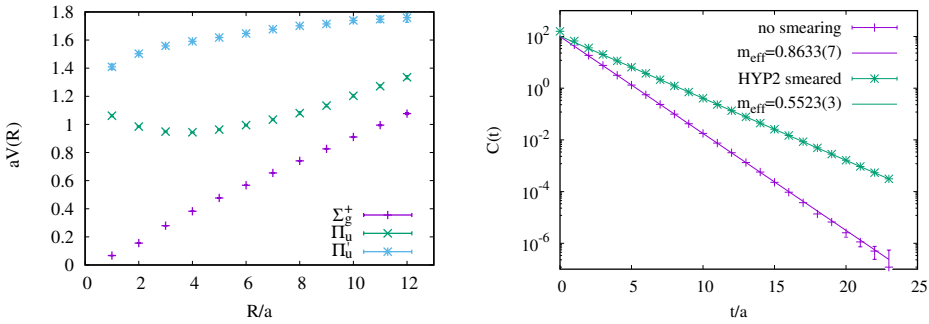

Fig. 4. The ground and first excited hybrid static potential for Π_u (left) together with the ground state static potential Σ_g^+ on a quenched ensemble and the static light meson correlator (right) on a $N_\mathrm{f} = 2$ Wilson fermion ensemble.

We can visualize a hybrid trial state via

$$\psi_{\Pi}^{(n)}(\vec{z},R) \;=\; \left\langle \sum_{\vec{k}\perp\vec{y}-\vec{x}} \left|\left| \sum_{i,j}^{N_v} \tilde{\rho}_{\Pi,R}^{(n)}(\lambda_i,\lambda_j) \left[\nabla_{\vec{k}} v_i(\vec{x}) v_i^\dagger(\vec{z}) v_j(\vec{z}) v_j^\dagger(\vec{x}+R) \right.\right.\right.$$
$$\left.\left.\left. + v_i(\vec{x}) v_i^\dagger(\vec{z}) v_j(\vec{z}) \left[\nabla_{\vec{k}} v_j\right]^\dagger (\vec{x}+R) \right] \right|\right|_2 \right\rangle . \tag{6}$$

4. The static-light (charm) meson operator

The static-light meson correlator reads

$$C(t) \;=\; \frac{1}{N_{\mathrm{f}}} \sum_{i,\vec{x},t_0} \left\langle \bar{Q}(\vec{x},t_0+t)\gamma_5 q^i(\vec{x},t_0+t) \bar{q}^i(\vec{x},t_0)\gamma_4\gamma_5 Q(\vec{x},t_0) \right\rangle , \tag{7}$$

with (infinitely) heavy (static) quarks Q and light-quark fields q^i of mass-degenerate flavors $i = 1 \ldots N_{\mathrm{f}}$. After Wick contraction, one finds

$$C(t) \;=\; -\sum_{\vec{x},t_0} \left\langle \mathrm{Tr}_{\mathrm{c,d}} \Big(\gamma_5 \underbrace{\mathcal{D}(\vec{x},t_0+t;\vec{x},t_0)\gamma_4}_{\text{light propagator}} \gamma_5 \underbrace{U_{\mathrm{t}}(\vec{x};t_0,t_0+t)P_-}_{\text{static propagator}} \Big) \right\rangle$$
$$= \; -\sum_{\vec{x},t_0} \left\langle \mathrm{Tr}_{\mathrm{c,d}} \Big(\mathcal{D}(\vec{x},t_0+t;\vec{x},t_0) P_+ U_{\mathrm{t}}(\vec{x};t_0,t_0+t) \Big) \right\rangle , \tag{8}$$

where the trace is taken over color and Dirac indices, with projectors $P_\pm = (1 \pm \gamma_4)/2$ and the temporal Wilson line $U_{\mathrm{t}}(\vec{x};t_0,t_0+t)$ of (time-like) HYP2 ($\alpha_{1,2,3} = 1, 1, 0.5$) fat links from $(\vec{x},t_0)$ to $(\vec{x},t_0+t)$. Using $k = 1 \ldots N_v$ Laplacian eigenvectors $v_k^c(\vec{x},t)$ and $\Omega^{-1} = D^{-1}\gamma_4$, we apply distillation [6]

$$C(t) = -\sum_{\vec{x},t_0,i,j} \left\langle \mathrm{Tr}_{\mathrm{c,d}} \left(\left[v_i \left(v_i^\dagger \Omega^{-1} v_j \right) v_j^\dagger \right] (\vec{x},t_0+t;\vec{x},t_0) P_+ U_{\mathrm{t}}(\vec{x};t_0,t_0+t) \right) \right\rangle$$
$$= -\sum_{t_0,i,j} \left\langle \mathrm{Tr}_{\mathrm{d}} \left\{ \left[v_i^\dagger \Omega^{-1} v_j \right] (t_0+t,t_0) P_+ \right\} \sum_{\vec{x}} \tau_{ij}(\vec{x},t_0,t_1) \right\rangle \tag{9}$$

with light (charm) perambulators $v^\dagger \Omega^{-1} v$ from [7], the projector P_+, and static perambulators $\tau_{ij}(\vec{x},t_0,t_0+t) = v_j^\dagger(\vec{x},t_0) U_{\mathrm{t}}(\vec{x};t_0,t_0+t) v_i(\vec{x},t_0+t)$ in Eq. (2), Section 1. The trace runs over color (c) and Dirac (d) indices. In the right plot of figure 4, we show the static–light (charm) correlator with and without HYP2 smearing of the temporal Wilson lines, the smearing drastically reduces the free energy and reveals the actual effective mass

of the system. The optimization of this operator using Gaussian profiles is underway. We can visualize a static-light meson state by removing the spatial sum in Eq. (9) and looking at individual contributions in the 3D spatial lattice volume

$$C(\vec{x},t) \;=\; -\sum_{t_0,i,j} \left\langle \mathrm{Tr_d} \left\{ \left[v_i^\dagger \Omega^{-1} v_j \right] (t_0+t,t_0) P_+ \right\} \tau_{ij}(\vec{x},t_0,t_0+t) \right\rangle . \quad (10)$$

5. Conclusions

We presented alternative creation operators for static-quark–anti-quark states based on Laplacian eigenmodes. Temporal correlations of the new operators are used to compute static quark–anti-quark ground and excited state potentials. One significant advantage of the approach is its efficiency for computing the static potential not only for on-axis, but also for many off-axis quark–anti-quark separations. We visualize the spatial distribution of the optimal Laplace trial states for ground and excited state creation operators of the quark–anti-quark pair. Further, we adapted the method to compute hybrid static potentials of exotic mesons, where gluonic string excitations are realized by covariant derivatives acting on the Laplacian eigenvectors. Finally, we showed how to combine the static and light quark perambulators to build a static-light quark meson.

The authors gratefully acknowledge the GCS (www.gauss-centre.eu) for computing time on SuperMUC-NG (www.lrz.de). The work is supported by the German Research Foundation (DFG) research unit FOR5269 "Future methods for studying confined gluons in QCD", and the MKW NRW under the funding code NW21-024-A. I thank my collaborators Francesco Knechtli, Tomasz Korzec, Mike Peardon, and Juan Andrés Urrea-Niño as well as Pedro Bicudo and Jeff Greensite for valuable discussions.

REFERENCES

[1] K.G. Wilson, *Phys. Rev. D* **10**, 2445 (1974).
[2] J. Greensite, *Prog. Part. Nucl. Phys.* **51**, 1 (2003), arXiv:hep-lat/0301023.
[3] R. Höllwieser *et al.*, *Phys. Rev. D* **107**, 034511 (2023), arXiv:2212.08485 [hep-lat].
[4] R. Höllwieser, F. Knechtli, M. Peardon, *PoS* **(LATTICE2022)**, 060 (2022), arXiv:2209.01239 [hep-lat].
[5] J.A. Urrea-Niño, F. Knechtli, T. Korzec, M. Peardon, *PoS* **(LATTICE2022)**, 087 (2022).
[6] Hadron Spectrum Collaboration (M. Peardon *et al.*), *Phys. Rev. D* **80**, 054506 (2009), arXiv:0905.2160 [hep-lat].
[7] F. Knechtli, T. Korzec, M. Peardon, J.A. Urrea-Niño, *Phys. Rev. D* **106**, 034501 (2022), arXiv:2205.11564 [hep-lat].